LUNAR LATITUDE AND TERRAIN RADIATOR SENSITIVITY STUDY

William Birmingham, Greg Schunk, Brian Evans
NASA Marshall Space Flight Center/ EV34 Thermal Analysis and Controls Branch/ ESSCA Contract/ Jacobs Space Exploration Group

ABSTRACT

The thermal environment on the moon is highly complex and diverse. The lunar surface near the equator develops extreme hot average temperatures during the lunar day due to solar flux vectors that are nearly orthogonal to the surface. The lunar poles have a cold and uniquely complex thermal environment with low solar elevation angles and permanently shadowed regions located just kilometers from some of the most highly illuminated regions of the moon. Likewise, the topography can range from very flat crater basins to dramatically tall features such as mountains and crater rims. Consequently, when sizing the radiators of a lunar surface vehicle, the specific thermal environment found in the targeted landing or deployment zone must be well understood to build robust appropriately scaled thermal control systems. Here described are parametric studies that characterize the sensitivity of lunar radiator performance to lunar terrain and latitude. Heat rejection is calculated for different radiator tilt angles in a variety of terrain environments. Radiator performance as a function of underside thermal condition is also characterized at lunar latitudes ranging from equatorial to polar. Impacts of latitude and terrain on radiator performance are quantified, and regions are identified where the thermal environment is more or less favorable for specific radiator designs.

NOMENCLATURE

α	Solar absorptivity
ε	Infrared emissivity
ε^*	Effective infrared emissivity
DSNE	Design Specification for Natural Environments
DXF	Drawing Exchange Format
FOV	Field of view
HLS	Human Landing System
LDEM	Lunar Digital Elevation Map
LTAG	Lunar Thermal Analysis Guidebook
MIT	Massachusetts Institute of Technology
MLI	Multilayer insulation
STK	System Tool Kit

INTRODUCTION

As the number of planned lunar missions continues to grow, so also does the need for early-stage mission planning tools. Performing detailed analysis is valuable and necessary to execute on any

lunar habitation or vehicle mission. However, the efficiency and potentially even the success of converging to a detailed design concept is predicated upon successful system-level scaling completed early in the mission planning phase. Thermal design is especially sensitive to early phase decision making due to the highly integrated nature of thermal systems. Under- or over-estimating mass, power, volume, or heat flow to the environment can have a significant impact on the size and type of thermal control needed. The goal of this analysis is to create a set of early design-phase radiator scaling tools for lunar habitations or vehicles given basic lunar environmental characteristics.

There are many complex environmental characteristics that impact thermal performance of lunar vehicles. For this assessment, two parameters are selected for their unique utility in sizing radiators: the relative terrain roughness and lunar latitude. The terrain effects captured in this assessment are the effects of warm lunar regolith within the view of the radiators due to the lunar habitat/vehicle's proximity to and tilt toward tall terrain features. Note that this study does not attempt to incorporate the effect of terrain blocking the sun at low solar elevation angles. The only terrain effects quantified in this study are the effects of direct terrain heating on the radiators. Lunar latitude affects local regolith temperature and solar flux on the radiators. Consequently, the effects of latitude are calculated for different underside radiator coatings. An important characteristic of this study is the effort to decouple the effects of terrain and latitude on radiator performance, assessing the impact of each parameter individually. Terrain is varied while maintaining one constant worst-case latitude assumption (~0° latitude), and latitude is varied while maintaining one constant terrain assumption (flat terrain). Also, given the vast quantities of data processing that would be required to assess every potential lunar surface mission site, the analysis to follow only attempts to capture maximum bounding effect of each of the above-described parameters.

LUNAR TERRAIN SENSITIVITY MODEL

To assess the sensitivity of radiators to lunar terrain, a parameter was defined for identifying lunar terrain samples of interest. The goal of this parameter is to scale the likelihood of tall terrain features entering the field of view (FOV) of upward facing radiators. The quantity selected to approximate this terrain characteristic is the standard deviation from local mean elevation. This parameter approximately correlates to the quantity and magnitude of elevation changes within a section of lunar terrain, effectively measuring the "roughness" of the local topography. The elevation data was obtained from a $1/512^{th}$ degree/pixel (~60m/pixel at the equator) resolution, cylindrical projection lunar elevation map. The maps were obtained from a Planetary Data System (PDS) node hosted by the Massachusetts Institute of Technology (MIT) [1]. Each standard deviation pixel was calculated using a block of 1280 by 1280 elevation pixels. This results in each pixel in the standard deviation map representing a ~76km by 76km section of lunar terrain (these dimensions are only accurate at the equator – pixels will be more distorted toward the poles). The full lunar map of local elevation standard deviation is shown in Figure 1.

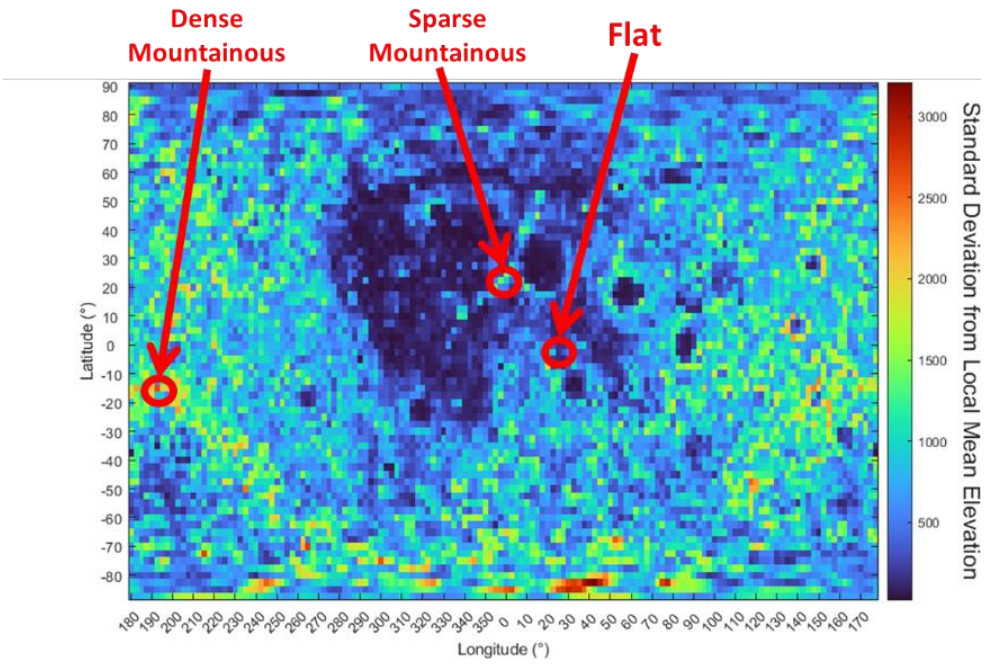

Figure 1. Standard deviation from mean local elevation, full lunar surface map. Selected terrain samples circled in red.

Using this parameterization tool, three sites were selected which represent various degrees of terrain "roughness" (i.e. local elevation standard deviation). The Apollo 11 landing site was found to be a suitable terrain sample representative for very flat terrain. This region has no features rising high enough to enter the FOV of upward-facing horizontal radiators and was found to be in the 9th percentile for terrain roughness on the lunar surface. The so called "sparse mountainous" terrain sample was chosen to be the Apollo 15 landing site. This site has a few terrain features tall enough to interact with the radiators but is located far enough away from these features to prevent radiative coupling to the regolith from dominating thermal behavior. This site was found to be in the 77th percentile in terms of terrain roughness. A terrain sample representing a dense mountainous environment was found on the far side of the moon. This site was chosen specifically for its extreme topography and was found to have a tall horizon surrounding the location on all sides. The site has nearby mountains rising 5km above the site, and the region around this site was found to be in the 99.8th percentile for roughness. (Note that the percentiles above are based on raw pixel counts of the cylindrical map projection, so terrain at the poles is over-represented in this calculation). The locations of these three samples are shown in Figure 1, and 3D renders of terrain are shown in Figure 2. Also, for reference, images of the Apollo 11 and 15 landing sites are shown in Figure 3 [2, 3].

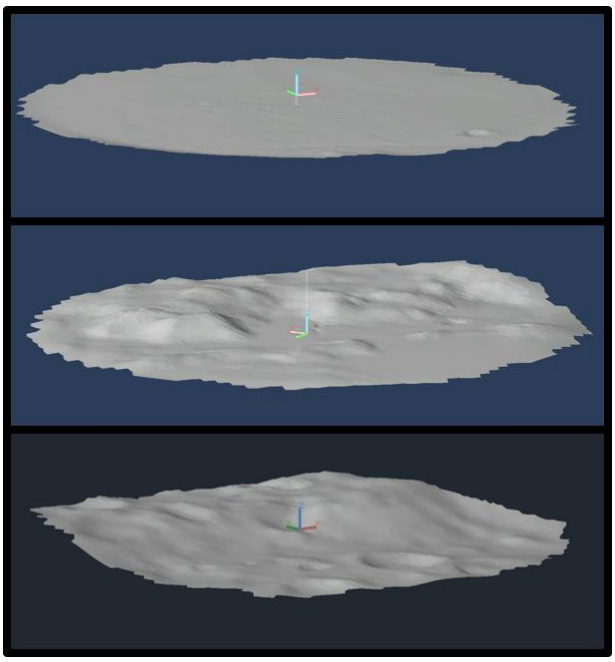

Figure 2. Terrain sample 3D renders. In order from top to bottom: flat terrain sample (Apollo 11 landing site), sparse mountainous terrain sample (Apollo 15 landing site), dense mountainous terrain sample (99.8th percentile roughness site).

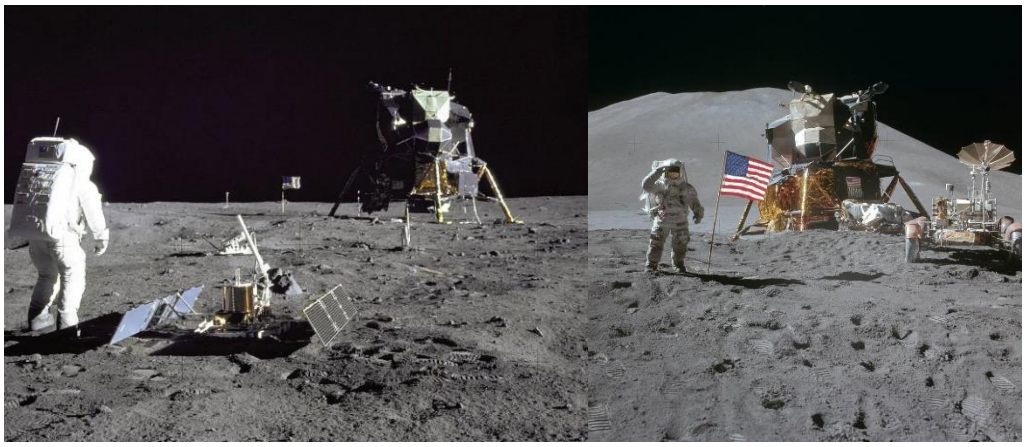

Figure 3. The Apollo 11 landing site (left) [2] and the Apollo 15 landing site (right) [3]

The lunar digital elevation maps (LDEM) of the three terrain samples were converted to Thermal Desktop models. This was done by converting the LDEM to a list of cartesian coordinates which, when formatted properly, can be uploaded into MeshLab, an open-source meshing software. Using methods and settings outlined in the Human Landing System (HLS) Lunar Thermal Analysis Guidebook (LTAG) [4], this list of cartesian coordinates can be converted to a mesh and saved as a DXF (Drawing Exchange Format) file which can then be imported into AutoCAD and converted to Thermal Desktop objects. From there, the thermophysical properties, optical properties, and orbits can be loaded to perform the analysis. For sparse and dense mountainous

terrain analysis, lunar highland optical and thermophysical properties are assumed for all cases due to the low likelihood of any tall terrain feature being composed of mare regolith. Mare optical properties are used for the Apollo 11 site. Per NASA's Cross-Program Design Specification for Natural Environments (DSNE), the highland optical properties used are: α/ε = 0.84/0.98, and the mare optical properties used are α/ε = 0.93/0.98 [5]. The regolith is modeled down to 2m as insulation nodes (within Thermal Desktop) using methods and thermophysical properties described in the LTAG [4]. For this analysis, the solar vector vs time was calculated using the System Tool Kit (STK) and uploaded into Thermal Desktop as a vector list. Note that in spite of each terrain sample being pulled from different latitudes and longitudes, the same solar path is used for all three samples to isolate the effects of terrain alone without the effect of solar flux variance. The solar vector list used for all three sites is calculated for a summer (solar maximum) day at the Apollo 11 landing site (which is less than 1° latitude from the equator).

The lunar module thermal model used for this analysis is shown in Figure 3. The module itself and the support legs are only intended to serve as stand-in structures to cast shadows and reflect heat onto the regolith and are not representative of any specific lander design. The arbitrary dimensions chosen for the lander are 4.5m diameter and 5m in height. A total of 6 radiators are used in this analysis, each with a single-sided surface area of $10m^2$ and each coated with an arbitrarily selected white, low solar absorptance radiator paint (α/ε = 0.09/0.91) [6]. The undersides of each radiator are inactive in the radiation calculation (effectively acting as an ideal MLI), and the temperatures of all 6 radiators are held constant at one of two set temperatures: 10°C or 60°C. 10°C is chosen to represent a typical average temperature for a crewed vehicle, and 60°C represents a radiator with a temperature lift (e.g., a heat pump) to increase heat rejection. Five of the radiators are tilted from 0° to 20° in 5° increments, and the sixth radiator is vertical. The thermal performance is assessed for tilted radiators to capture the effects of a structure that is sitting on uneven terrain or the effect of sub-optimal radiator deployment. The four radiators with a non-zero, non-vertical tilt are pointed eastward because in both the sparse and dense mountainous terrain samples, the tallest terrain features are located east of the module.

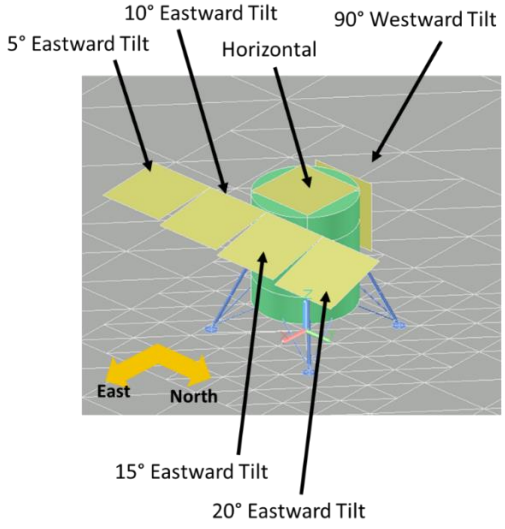

Figure 3. Lunar module thermal model for the terrain sensitivity study.

RADIATOR SENSITIVITY TO TERRAIN ROUGHNESS AND RADIATOR TILT

For each terrain sample, the model was run for 2 years to achieve quasi-steady-state temperatures on the surface (longer model runs are required to achieve quasi-steady-state of deeper regolith layers). After the 2-year initializer run, the model is run for a single lunar sidereal day, and the heat rejection vs time is calculated for each of the 6 radiators. Figure 4 shows heat rejection vs time for all three terrain samples and both temperature settings. As the sun rises, the radiator heat rejection slowly decreases until peak solar heating occurs, after which the heat rejection increases again as the sun sets. For the sparse and dense mountainous terrain samples, the heat rejection drops quickly shortly after the sun rises. This is due to the sun being obscured by terrain early in the morning and the radiators quickly heating after the sun rises over the surrounding mountains. Using these curves, the minimum heat rejection can be determined, and this is used as the characteristic worst-case heat rejection. The most ineffective radiator behavior seen for each case is that of the vertical radiator which is coupling so strongly to the surrounding hot regolith that negative heat rejection (or positive net heat absorption) is observed.

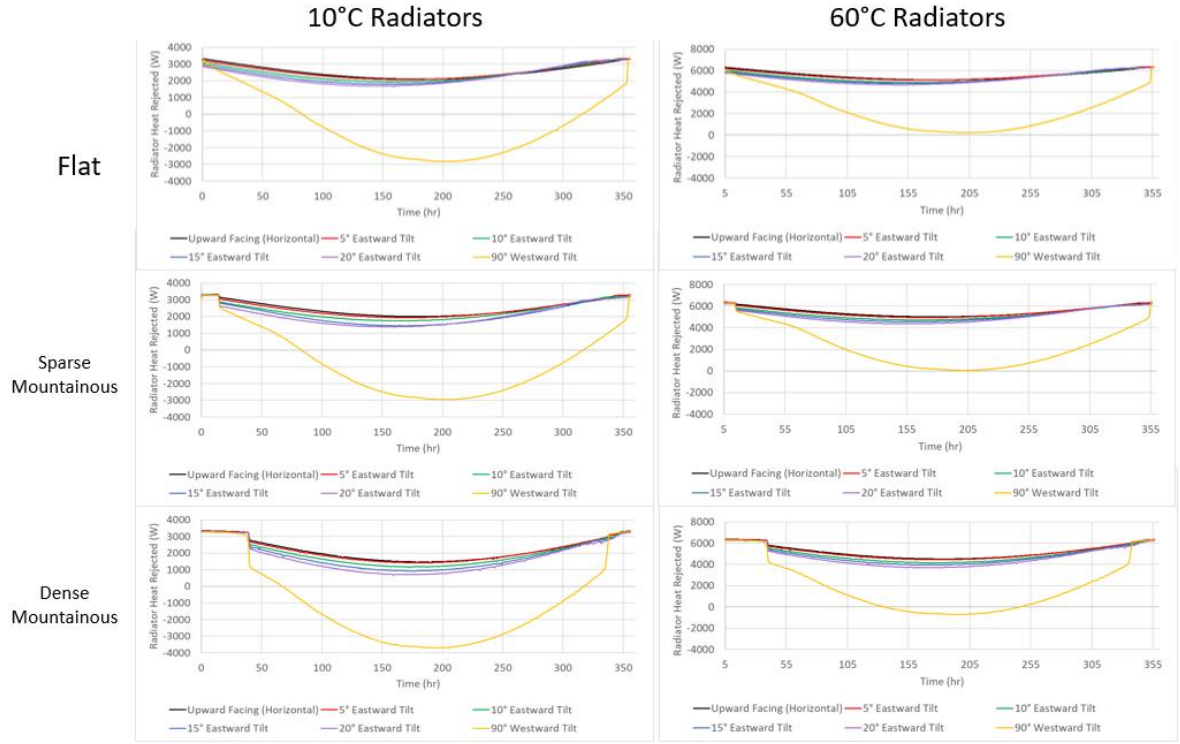

Figure 4. Radiator heat rejection vs time. In order from top to bottom: flat terrain sample (Apollo 11 landing site), sparse mountainous terrain sample (Apollo 15 landing site), dense mountainous terrain sample (99.8th percentile roughness site). Left to Right: Data for 10°C radiators, data for 60°C radiators.

Table 1 shows the impact of terrain for a sparse mountainous environment, and Table 2 shows the terrain effects for a dense mountainous environment. For sites with sparse mountainous terrain, thermal impacts can be modest, causing radiator performance degradation by 6% for a

perfectly horizontal radiator. Sparse mountainous terrain coupled with a 20° tilt, however, caused radiator performance to degrade by 34-37% (depending on the set temperature) compared to a horizontal radiator on flat terrain. In an extreme worst-case hot scenario, highly mountainous terrain can have a significant impact on radiator performance, causing radiator performance degradation of up to 31% for a perfectly horizontal radiator and between 68% & 70% for a 20° tilted radiator.

Table 1. Terrain Induced Radiator Performance Degradation for 10°C Radiators

Ideal, Flat Terrain, Horizontal Radiator Heat Rejection (Control): $210 W/m^2$	Flat Terrain: Percent Radiator Heat Rejection Decrease Due to Tilt Alone	Sparse Mountainous Terrain: Percent Radiator Heat Rejection Decrease Due to Terrain and Tilt	Dense Mountainous Terrain: Percent Radiator Heat Rejection Decrease Due to Terrain and Tilt
Horizontal Radiator	N/A	6%	30%
5° Eastward Tilt	1%	9%	33%
10° Eastward Tilt	8%	17%	46%
15° Eastward Tilt	14%	25%	55%
20° Eastward Tilt	21%	34%	68%

Table 2. Terrain Induced Radiator Performance Degradation for 60°C Radiators

Ideal, Flat Terrain, Horizontal Radiator Heat Rejection (Control): $513 W/m^2$	Flat Terrain: Percent Radiator Heat Rejection Decrease Due to Tilt Alone	Sparse Mountainous Terrain: Percent Radiator Heat Rejection Decrease Due to Terrain and Tilt	Dense Mountainous Terrain: Percent Radiator Heat Rejection Decrease Due to Terrain and Tilt
Horizontal Radiator	N/A	2%	13%
5° Eastward Tilt	0.4%	4%	13%
10° Eastward Tilt	4%	8%	19%
15° Eastward Tilt	6%	11%	23%
20° Eastward Tilt	9%	15%	29%

These degradation factors allow for quick worst-case approximations of terrain effects on a 10°C or 60°C radiator given the performance of the ideal case is known. For example, if a 10°C radiator is calculated to reject 100W in a simplified case with no terrain effects, it is reasonable

to conclude that with the addition of terrain effects, heat rejection is unlikely to ever degrade to less than 68W if the radiator can remain horizontal. Non-equatorial sites will on average have reduced regolith temperatures, resulting in a reduced impact from terrain. Consequently, since the data in Tables 1 & 2 are calculated at the equator, they report worst-case performance degradation. It is important to note that this data was obtained only for 10°C and 60°C radiators. A radiator with a temperature outside of this range will require extrapolation to estimate performance degradation.

LUNAR LATITUDE SENSITIVITY MODEL

Another consideration important for successful radiator scaling relates to how radiator performance changes with latitude. The farther from the equator the lunar module/vehicle is located, the shallower the elevation angle of the sun will be at lunar noon. Shallower solar elevation angles result in a decreased solar flux on the radiators as well as decreased average regolith temperatures. Thus, the goals of this part of the study are to determine how maximum heat rejection capacity of horizontal radiators changes with latitude, and to assess how underside coatings on deployable horizontal radiators affect radiator performance at different latitudes. The underside coating of horizontal radiators can increase or decrease radiative coupling to the regolith which can increase or decrease heat rejection capacity. To assess the sensitivity of radiator performance to lunar latitude alone, the analysis to follow decouples latitude effects from location-specific terrain effects by using a perfectly flat disk to represent regolith. All analysis cases are run from 0° latitude to 90°South latitude in 10° increments. The regolith disk diameter is 200m which was calculated to achieve an equivalent to 95% of the module's view factor to an infinite plane.

The thermal model used to represent the lunar module is shown in Figure 5. The model of the primary structure is the same as that used for the terrain sensitivity thermal analysis and only exists to cast shadows and reflect heat onto the regolith. Like the terrain sensitivity study, two radiator temperatures are considered: 10°C and 60°C. Four cantilevered, $10m^2$, deployable horizontal radiators are included in the analysis, each with the same radiator paint used for the terrain analysis applied to the top side, and each with a different underside coating. The gray radiator shown in Figure 5 has an adiabatic boundary on the underside (used as a control surface), the red radiator has a multilayer insulation (MLI) covering ($\varepsilon^* = 0.01$) on the underside, the green radiator has white radiator paint on both sides, and the blue radiator has a low infrared emissivity coating ($\alpha/\varepsilon = 0.24/0.04$) on the underside. The goal of analyzing these different underside conditions is to determine latitude ranges in which different radiator designs are applicable.

Also shown in Figure 5 are the two analyzed radiator configurations. The side of the vehicle with the greatest sun exposure at noon will reflect heat onto the regolith which will impose a greater infrared heat load on the underside of the radiators located on that side. Since this analysis only looks at cases in the southern hemisphere, the north side of the vehicle receives the most sun in almost all cases, and consequently radiators reject less heat on this side. The two configurations shown are clocked to ensure all 4 radiators are assessed in the worst-case configuration.

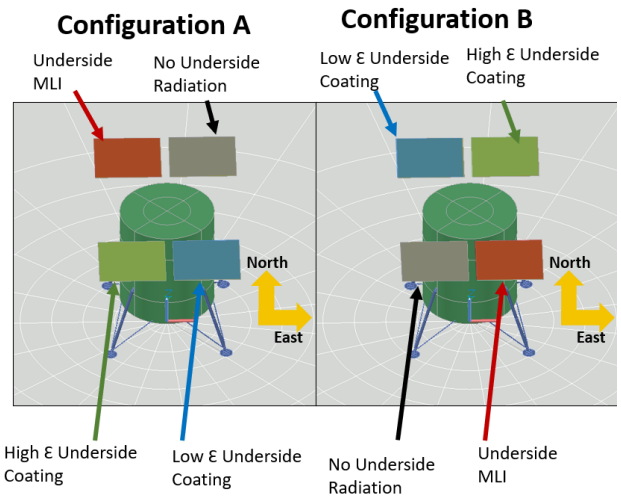

Figure 5. Lunar module thermal model for the latitude sensitivity study.

The study was composed of 80 cases. Cases were analyzed for all 10 latitudes for each of the two radiator configurations (though only worst-case configuration data is shown below) at two set temperatures (10°C and 60°C) and using regolith optical properties of both highland and mare regolith.

RADIATOR SENSITIVITY TO LATITUDE AND UNDERSIDE COATING

The heat rejection capacity of a radiator will increase at latitudes closer to the poles due to the shallower angle of the sun reducing the heat load on the radiators. Table 3 shows ideal top side heat rejection as a function of latitude. Regardless of radiator temperature, an ideal upward facing radiator can reject 122 W/m^2 more at the south pole than it can at the equator.

Table 3. Minimum Top Side Radiator Heat Rejection vs Lunar Latitude

Latitude (°)	Minimum (Noon) Topside Heat Rejection for a 60°C Radiator (W/m^2)
0	513
-10	515
-20	521
-30	530
-40	543
-50	558
-60	575
-70	594
-80	615
-90	635

Tables 4 and 5 show the maximum radiator performance degradation as a function of latitude for 10°C and 60°C radiators respectively. For radiators with an MLI underside covering, modest performance degradation is observed in all cases. The highest degradation was found to be 3.6%

for a 10°C radiator near the equator, on Mare regolith. The radiators with a low emissivity underside coating show high magnitude noise in the heat rejection vs latitude data. This is due to a need for lower error tolerance in the radiation calculation and, consequently, a need for significantly greater computation time. While this data is ultimately inconclusive, it gives an order of magnitude approximation for performance degradation expected for this underside coating. The performance of a radiator with a high emissivity underside coating (i.e. a double-sided radiator) shows a strong dependence on lunar latitude. For 10°C radiators over Mare regolith, latitudes north of ~61° South (interpolated) show greater than 100% performance degradation, indicating the radiator is absorbing rather than rejecting heat. For 60°C radiators, there is no latitude at which heat absorption is observed. For 10°C radiators over Mare regolith, latitudes south of ~77° south (interpolated) show negative performance degradation, indicating the underside coating is increasing heat rejection capacity compared to a top-side only radiator. For 60°C radiators, improved heat rejection is observed south of the ~60° south latitude line.

Table 4. Radiator Performance Degradation Vs Latitude for 10°C Radiators

Latitude	**Worst Case Performance Degradation Due to Latitude and Underside Condition: MLI Underside Covering**		**Worst Case Performance Degradation Due to Latitude and Underside Condition: Low Emissivity Underside Coating**		**Worst Case Performance Degradation Due to Latitude and Underside Condition: High Emissivity Underside Coating**	
	Highland	**Mare**	*Highland**	*Mare**	**Highland**	**Mare**
0°	**3.1%**	**3.5%**	*30.6%*	*30.0%*	**286.0%**	**326.4%**
-10°	**3.1%**	**3.6%**	*35.8%*	*31.0%*	**288.8%**	**326.4%**
-20°	**3.1%**	**3.5%**	*36.1%*	*25.8%*	**280.4%**	**317.6%**
-30°	**2.8%**	**3.1%**	*30.1%*	*26.1%*	**255.1%**	**288.8%**
-40°	**2.3%**	**2.6%**	*28.2%*	*25.0%*	**208.5%**	**234.1%**
-50°	**1.7%**	**1.9%**	*23.5%*	*19.9%*	**151.9%**	**173.8%**
-60°	**1.0%**	**1.2%**	*19.8%*	*16.0%*	**92.0%**	**108.8%**
-70°	**0.4%**	**0.5%**	*14.7%*	*13.1%*	**33.4%**	**44.2%**
-80°	**-0.3%**	**-0.2%**	*8.3%*	*9.3%*	**-23.0%**	**-17.6%**
-90°	**-0.8%**	**-0.8%**	*7.4%*	*6.9%*	**-72.6%**	**-72.0%**

** Low emissivity performance degradation data is inconclusive due to the noise observed.*

Table 5. Radiator Performance Degradation Vs Latitude for 60°C Radiators

Latitude	Worst Case Performance Degradation Due to Latitude and Underside Condition: MLI Underside Covering		Worst Case Performance Degradation Due to Latitude and Underside Condition: Low Emissivity Underside Coating		Worst Case Performance Degradation Due to Latitude and Underside Condition: High Emissivity Underside Coating	
	Highland	Mare	*Highland**	*Mare**	Highland	Mare
0°	0.6%	0.8%	*10.5%*	*8.9%*	59.4%	75.7%
-10°	0.7%	0.8%	*12.7%*	*10.2%*	61.3%	76.8%
-20°	0.6%	0.8%	*13.1%*	*7.5%*	60.4%	75.7%
-30°	0.6%	0.7%	*9.9%*	*8.7%*	53.3%	67.8%
-40°	0.4%	0.5%	*10.2%*	*9.3%*	37.4%	48.8%
-50°	0.2%	0.3%	*8.1%*	*6.4%*	16.2%	26.2%
-60°	-0.1%	0.0%	*7.2%*	*4.9%*	-7.8%	-0.2%
-70°	-0.4%	-0.3%	*4.9%*	*4.5%*	-33.3%	-28.0%
-80°	-0.7%	-0.6%	*1.1%*	*2.8%*	-59.5%	-56.8%
-90°	-0.9%	-0.9%	*1.9%*	*1.6%*	-84.2%	-83.9%

** Low emissivity performance degradation data is inconclusive due to the noise observed.*

Figure 6 plots raw worst-case heat flux from double-sided and MLI-backed radiators as a function of latitude. This trade, comparing the two radiator underside conditions, shows that double-sided 10°C radiators perform better (i.e. reject more heat) than MLI-backed radiators south of the 76° south latitude line. Double-sided 60°C radiators perform better than MLI-backed radiators south of the 60° south line.

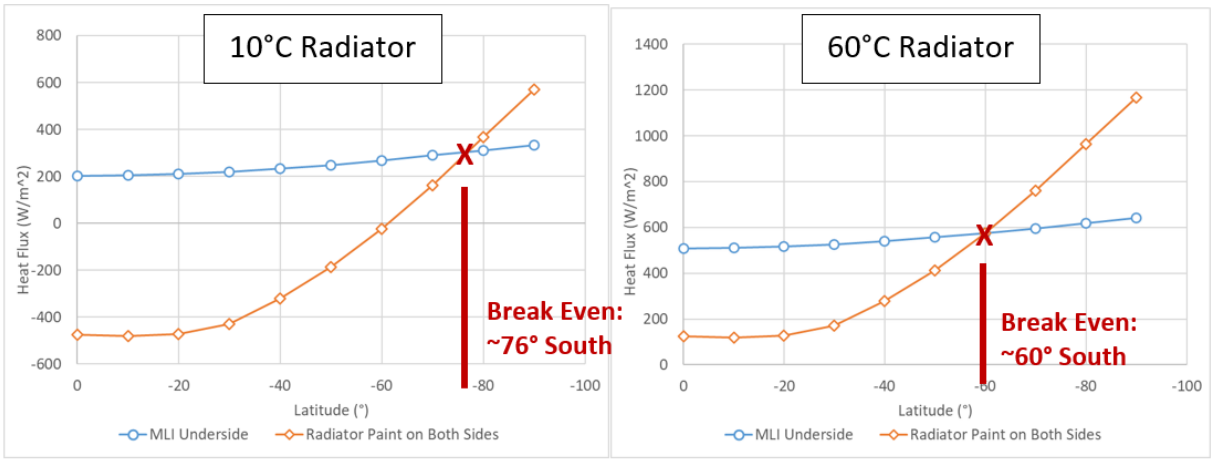

Figure 6. Worst case radiator heat rejection vs latitude with MLI applied to the underside and Radiator paint applied to both sides. The radiator is 10°C (left) and 60°C (right)

CONCLUSIONS

The terrain effects study shows potential for a substantial (32%) decrease in radiator heat rejection capacity in the most extreme terrain environments. Even greater degradation (68%) is observed with radiators tilted up to 20° toward the extreme terrain features. However, sparse mountainous terrain, which is considerably more common, has a more modest impact on thermal performance, causing 6% and 37% performance degradation for 0° tilt and 20° tilt respectively. The terrain effects study also shows radiator performance reduction is minimally affected by radiator temperature, with the 10°C radiator and 60°C radiator cases showing similar degradation factors. The latitude sensitivity study shows an increase of 122 W/m^2 in the heat rejection capacity of ideal horizontal radiators located at the poles compared to that of radiators located on the equator. MLI was found to be an effective underside insulator even for extreme equatorial environments, resulting in a maximum degradation of 3.6%. Further work must be done to assess the effects of low emissivity underside coatings on lunar radiator performance. The effect of adding highly emissive radiator paint to the underside of the radiators was found to have a strong dependence on lunar latitude. Closer to the equator, the detrimental effect on radiator performance is so great that the radiator absorbs heat at the 10°C setpoint. Closer to the poles, coupling to the cold regolith caused an improvement in radiator performance for both radiator set temperatures.

Because the two studies were decoupled, degradation factors for latitude and terrain can be applied independently or stacked to estimate the worst-case effects of each parameter on radiator performance anywhere on the lunar surface. Note, however, that terrain degradation factors will become more and more conservative the closer the site is located to the poles. In addition to the data generated for this study, the analysis methods employed to obtain the degradation factors and latitude ranges are also of use. The results shown above are only applicable to a specific set of radiator designs: horizontal deployable radiators between 10°C and 60°C. The work described here could be expanded to perform sensitivity studies that include vertical radiators, unique terrain environments, dust effects, different set temperatures, etc. While these approximation tools are not a replacement for detailed analysis and will tend toward conservatism, they provide a fast-turnaround design assessment capability that can speed up and improve the accuracy of early mission phase thermal system scaling.

REFERENCES

[1] LOLA PDS Data Node. (n.d.). MIT. Retrieved March 26, 2024, from https://imbrium.mit.edu/

[2] Apollo 11 - NASA. (n.d.). NASA. Retrieved August 7, 2024, from https://www.nasa.gov/gallery/apollo-11/page/2/

[3] Apollo 15 - NASA. (n.d.). NASA. Retrieved August 7, 2024, from https://www.nasa.gov/gallery/apollo-15/

[4] Human Landing System Lunar Thermal Analysis Guidebook. (2021). National Aeronautics and Space Administration, Baseline Release. https://ntrs.nasa.gov/api/citations/20210010030/downloads/HLS-UG-001%20Lunar%20Thermal%20Analysis%20Guidebook%20Baseline_STI.pdf

[5] Roberts, B. (2019). Cross Program Design Specification for Natural Environments (DSNE), NASA Technical Reports Server. https://ntrs.nasa.gov/citations/20200000867

[6] AZW/LA-II Ultra-Low Solar Absorptance White Thermal Control Paint / Coating. (n.d.). AZ Technology LLC. Retrieved August 5, 2024, from https://www.aztechnology.com/product/2/azw-la-ii